AIP | Review of Scientific Instruments

# Impact of x-ray dose on the response of CR-39 to 1–5.5 MeV alphas

J. Rojas-Herrera, H. G. Rinderknecht, A. B. Zylstra, M. Gatu Johnson, D. Orozco, M. J. Rosenberg, H. Sio, F. H. Seguin, J. A. Frenje, C. K. Li, and R. D. Petrasso

Citation: Review of Scientific Instruments **86**, 033501 (2015); doi: 10.1063/1.4913906
View online: http://dx.doi.org/10.1063/1.4913906
View Table of Contents: http://scitation.aip.org/content/aip/journal/rsi/86/3?ver=pdfcov
Published by the AIP Publishing



# Impact of x-ray dose on the response of CR-39 to 1–5.5 MeV alphas

J. Rojas-Herrera,[a] H. G. Rinderknecht, A. B. Zylstra, M. Gatu Johnson, D. Orozco, M. J. Rosenberg, H. Sio, F. H. Seguin, J. A. Frenje, C. K. Li, and R. D. Petrasso
*Plasma Science and Fusion Center, Massachusetts Institute of Technology, Cambridge, Massachusetts 02139, USA*

(Received 11 December 2014; accepted 18 February 2015; published online 4 March 2015)

The CR-39 nuclear track detector is used in many nuclear diagnostics fielded at inertial confinement fusion (ICF) facilities. Large x-ray fluences generated by ICF experiments may impact the CR-39 response to incident charged particles. To determine the impact of x-ray exposure on the CR-39 response to alpha particles, a thick-target bremsstrahlung x-ray generator was used to expose CR-39 to various doses of 8 keV Cu-$K_\alpha$ and $K_\beta$ x-rays. The CR-39 detectors were then exposed to 1–5.5 MeV alphas from an Am-241 source. The regions of the CR-39 exposed to x-rays showed a smaller track diameter than those not exposed to x-rays: for example, a dose of 3.0 ± 0.1 Gy causes a decrease of (19 ± 2)% in the track diameter of a 5.5 MeV alpha particle, while a dose of 60.0 ± 1.3 Gy results in a decrease of (45 ± 5)% in the track diameter. The reduced track diameters were found to be predominantly caused by a comparable reduction in the bulk etch rate of the CR-39 with x-ray dose. A residual effect depending on alpha particle energy is characterized using an empirical formula. © *2015 AIP Publishing LLC.* [http://dx.doi.org/10.1063/1.4913906]

## I. INTRODUCTION

In many scientific disciplines, including Inertial Confinement Fusion (ICF) research, charged particles and neutrons are often studied with solid-state nuclear track detectors (SSNTD).[1–12] These are crystal or polymer materials in which ionizing nuclear particles leave detectable *tracks* of molecular damage sites.[3–5] CR-39, a transparent SSNTD with chemical composition $C_{12}H_{18}O_7$, is particularly well suited for detecting nuclear particles because its induced tracks are revealed optically by etching with sodium hydroxide. These tracks can then be identified with an optical microscope with 100% efficiency for many charged particles that are normally incident to its surface (such as protons in the energy range 0.5–8 MeV[4,6]). The uniquely high sensitivity of CR-39 has made it the detector of choice for light ion studies because the ionization levels of protons and deuterons are typically below the response thresholds of other detectors.[9]

Previous work with various types of CR-39 has studied the effectiveness of track etchants[10] and has looked at CR-39 response to electrons,[3] neutrons,[11] protons,[7] deuterons,[13] tritons,[13] and alpha particles.[9] One thing that has not been quantitatively studied is how the CR-39 response to these particles is modified when the CR-39 is exposed to high fluence of x-rays, as it is when used in experiments at ICF facilities like OMEGA[14] and the NIF,[15] where doses of close to 5 Gy are typical.

In this paper, we present a comparison of the response to alpha particles of TasTrak® CR-39[16] with and without exposure to x-rays. The theory of track formation in CR-39 is discussed in Sec. II. Section III presents the methodology and results. Finally, the effect of x-ray dose on the response to alpha particles as a function of both energy and x-ray dose are presented in Sec. IV, and summarized in Sec. V.

## II. THEORY

Charged particles traveling through the CR-39 material deposit energy in the plastic through Coulomb scattering with electrons, leaving trails of damaged polymer chains.[18] When the plastic undergoes chemical etching, the broken molecular chains and free radicals become the seeds for the formation of conical pits or "tracks." The geometry of these tracks is dictated by the simultaneous action of two etching processes: chemical dissolution along the track (track etch rate $v_t$) and general dissolution on the etched surface (bulk etch rate $v_b$).[2] The sensitivity of CR-39 is defined by the ratio of track to bulk etch rates as described by

$$\frac{v_t}{v_b} = 1 + k\left(\frac{dE/dx_{elec}}{[keV/\mu m]}\right)^n, \tag{1}$$

where $k$ and $n$ are constants.[19] Typical values of $k$ and $n$ are 0.002 and 1.9, respectively.[17] Here and throughout the paper, calculations involving the stopping power $dE/dx$ are in units of keV/$\mu$m. Electronic stopping power is used, rather than the total stopping power, since the collisions with the electrons produce most of the ionization responsible for the molecular damage. $(dE/dx)_{elec}$ is determined from the ion stopping code SRIM[6] (Fig. 1). The range of 5.5 MeV alpha particles in CR-39 is approximately 44 $\mu$m.

If we consider the case of normal alpha incidence on the CR-39, simple geometry gives an analytical expression[2] for the track diameter ($D$):

$$D = 2v_b t\sqrt{\frac{v_t/v_b - 1}{v_t/v_b + 1}}, \tag{2}$$

[a]Electronic mail: jimmy06@mit.edu

 

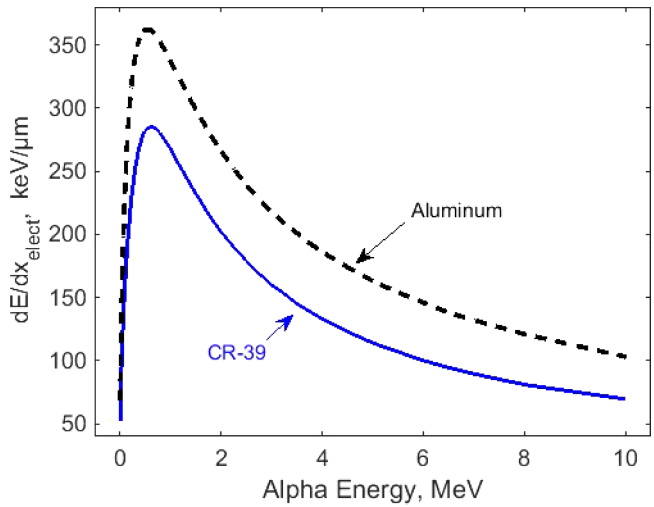


FIG. 1. Stopping power for alphas with energies in the range of 0-10 MeV in CR-39. This function is used to calculate the $v_t/v_b$ ratio given by Eq. (1). As a reference, the stopping power for alphas in aluminum is also plotted for the same energy range. Values obtained from SRIM.[6]

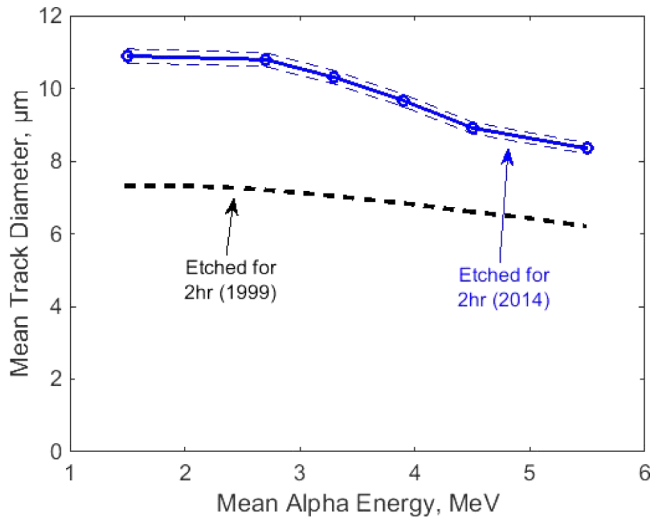


FIG. 3. Alpha track diameter and standard deviation as a function of mean energy for TasTrak® CR-39. Blue data were obtained from these experiments; for comparison, the measured data from the same experiment performed in 1999 by Hicks is also shown (black).[17] As will be discussed, this ~33% difference is due to the change in the chemistry of the material (and therefore its etch rate) over the years.

where $t$ is the etch time. Based on Eqs. (1) and (2), x-ray exposure could modify the sensitivity of the CR-39 through changing the bulk etch rate, track etch rate, or both. Combining Eqs. (1) and (2) gives an equation of $D$ as a function of the etch time, bulk etch rate, and stopping power

$$D = 2v_b t\left(\frac{2}{k\left(\frac{dE}{dx}\right)^n} + 1\right)^{-0.5}. \quad (3)$$

As a reference, Fig. 3 shows the mean track diameter as a function of alpha particle energy after a 2 h etch when no x-rays are applied to the piece. Equation (3) correctly explains this behavior for $k = 0.002$ and $n = 1.9$, as suggested in the literature.[17]

In the limit where $k(dE/dx)^n \gg 2$ (that is to say $v_t/v_b \gg 1$), the mean track diameter becomes independent of $dE/dx$ and $D \approx 2v_b t$. For particles with large stopping powers, track diameters all saturate at a maximum value set by the bulk etch rate only (assuming that $t_{etch}$ was carefully selected to avoid tracks from etching out). This behavior can be observed in the 1.5 and 2.7 MeV points in Fig. 3, for which the diameter has saturated at a maximum value (11 $\mu$m). In fact, the stopping power of the alpha particles in CR-39 continues to grow as alpha energy is reduced, until it peaks at around 0.7 MeV (see Fig. 1). The alpha energies studied in this work, therefore, probe the high-stopping-power limit. This feature, and a study of the bulk etch rate directly by measuring the volume and mass of the CR-39 before and after etching, is essential for understanding how x-rays impact the CR-39 sensitivity to particles.

## III. EXPERIMENTAL RESULTS

### A. Experimental study of track diameter versus x-ray dose

The experimental setup is shown in Fig. 2. CR-39 pieces (1.5 mm thick and 5 cm diameter) were exposed to different x-ray doses defined by several filters positioned as shown

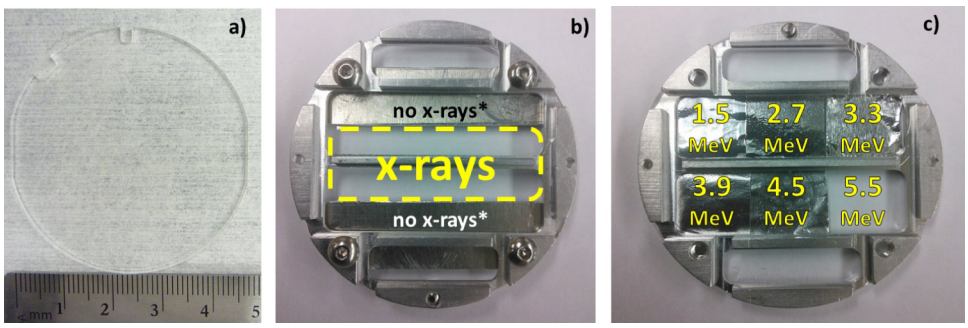


FIG. 2. (a) A typical sample of 5-cm diameter, 1.5-mm-thick CR-39 used in this study. (b) The x-ray shielding mask used in this study: two 1 mm thick aluminum plates cover half of each mask window (labeled with an asterisk in the figure). The aluminum shield effectively blocks the 8 keV x-rays, transmitting only $10^{-6}$ of the incident intensity. (c) Alpha particle range filters used in the study. Six different alpha energies were obtained on the CR-39 by ranging down 5.5 MeV alphas from an Am-241 source using different aluminum filters. With this combination of x-ray and alpha filters, 12 regions of data were obtained on each CR-39 sample: x-ray-exposed and unexposed regions for each of 6 alpha particle energies. The area covered with aluminum between the two main windows provides a small background region on the CR-39. Each piece was then etched for 2 h in an 80 °C solution of 6 M NaOH.

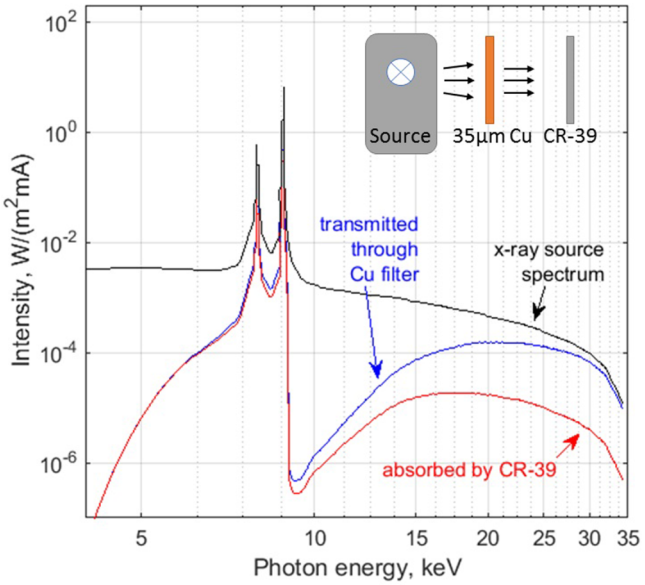


FIG. 4. Spectral intensity of the x-ray source (black), the intensity transmitted through 35 $\mu$m Cu filtering (blue), and the intensity absorbed by the CR-39 (red). The inset cartoon shows the experimental layout used. The thick Cu-target bremsstrahlung x-ray source was run with a voltage of 35 kV and a current of 18 mA. 91% of the absorbed energy was from the Cu-K$_\alpha$ and K$_\beta$ lines radiation (8–9 keV).

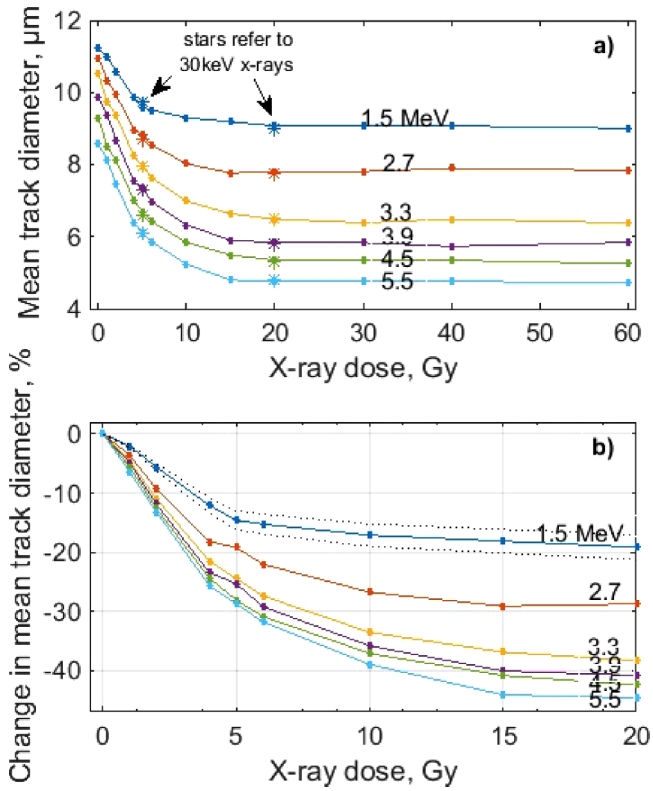


FIG. 5. (a) Alpha track diameter as a function of x-ray dose and alpha incident energy. A characteristic uncertainty (from repeatability experiments) of track diameter of less than 3% (comparable to the size of the points) was observed in each case. For a given alpha energy, track diameter decreases linearly with x-ray doses up to 5 Gy, and then approaches an asymptotic non-zero value for doses of 20 Gy and above. Experiments depositing 5 and 20 Gy using a different (~30 keV) x-ray source (*stars*) show that the observed behavior appears to be independent of photon energy. (b) Percentage change of mean track diameter for each alpha energy as a function of dose. The standard deviation corresponds to approximately 10% of each value, but it is only plotted for the 1.2 MeV case for clarity (dotted lines). All samples were etched for 2 h in an 80 °C solution of 6 M NaOH. The changes in mean track diameter shown in these figures were observed in CR-39 samples that were exposed and then stored up to 1 week before etching; the effect of longer periods between exposure and etching remains to be studied.

in the figure. The x-ray irradiation was performed using a thick-target bremsstrahlung x-ray machine (Philips Electronic Instruments X-ray Generator). This x-ray machine emits the spectrum shown in Fig. 4, including both line radiation and bremsstrahlung components. A 35 micron Cu filter was positioned between the source and the CR-39 to isolate the 8.0 keV Cu-K$_\alpha$ and 8.9 keV Cu-K$_\beta$ lines: 91% of the energy absorbed by the CR-39 was from this line radiation. Radiochromic film (RCF) was used to measure the incident intensity of x-rays in the sample plane.[20] An average intensity was found, and was used to calculate the dose per unit time in the CR-39 pieces. Additionally, a surface barrier detector (SBD) was used to account for fluctuations in machine power output during the exposure. A second generator producing a broadband spectrum with a maximum of 225 keV and a peak intensity at ~30 keV was used to evaluate the impact of photon energy on changes in the CR-39 response.

Each piece was then exposed to alphas from a 0.1 $\mu$Ci Am-241 alpha source (placed 9 cm away from the CR-39), which produced an approximate fluence of 15 000 alphas per cm$^2$. The 5.48 MeV alphas produced by the source were ranged down by a set of aluminum filters to obtain different energies of particles on the CR-39, as shown in Fig. 2. The x-ray- and alpha- exposed regions were overlapped such that each region with a particular alpha energy contained both x-ray exposed and unexposed portions. In total, 35 different experiments were conducted with various doses of x-rays from 0 to 60 Gy, including repeatability tests.

After exposure, the samples were all etched for 2 h in an 80 °C solution of 6 M NaOH. An automated optical microscope system was used to scan each CR-39 sample and record individual track information (diameter, contrast, and uncertainty) for later analysis.[13]

The mean alpha track diameters were observed to decrease with increased x-ray dose, as illustrated in Fig. 5. The mean track diameters are reduced roughly linearly with x-ray dose below 5 Gy, and approach an asymptotic value for doses of 20 Gy and above. The percentage change in the mean track diameter for each alpha energy as a function of dose is shown in Fig. 5(b). From this graph, for example, we can observe that if the piece of CR-39 is exposed to 4 Gy, a 1.5 MeV alpha will produce a track with a diameter that is smaller than normal by 12% ± 1%.

### B. Experimental measurement of the Bulk etch rate versus x-ray dose

Given the track diameter versus x-rays dose behavior shown in Fig. 5(a), we assumed that this trend was due to changes in the bulk etch rate as given by Eq. (3). As a result, the following $v_b$ measurements were performed to investigate this hypothesis. The bulk etch rate was determined directly by measuring the change of CR-39 thickness before and after

etching. An optical microscope was used to find this thickness by finding the difference in the height of the optical stage between focusing on the front and the back surfaces of the piece (optical thickness or Δz). The optical thickness is related to the true thickness by a function dependent on the index of refraction, $f(n)$. True thickness is defined as $d = \Delta z f(n)$. The bulk etch rate is given by[2]

$$v_b = \frac{d_f - d_i}{2t_{etch}} = \frac{\Delta z_f - \Delta z_i}{2t_{etch}} f(n), \tag{4}$$

where $\Delta z_f$ and $\Delta z_i$ are the final and initial optical thicknesses. A piece of CR-39 was divided into 3 sections, each exposed to a different x-ray dose. An unexposed region was measured as well for background reference. The optical thickness and the X and Y coordinates were recorded at the 18 regions measured in every piece. The piece was then etched for 5 h, and the optical thickness was determined again in the locations previously recorded. This method allowed us to find a ratio between $v_b(X)$ (bulk etch rate of regions exposed to x-rays) and $v_b(0)$ (bulk etch rate of regions unexposed to x-rays), which is independent of the index of refraction:

$$\frac{v_b(X)}{v_b(0)} = \frac{(\Delta z_f - \Delta z_i)_X}{(\Delta z_f - \Delta z_i)_0}, \tag{5}$$

where the subscripts $X$ or $0$ again indicate regions exposed or not exposed to x-rays. The observed ratio of $v_b(X)$ to $v_b(0)$ is shown in Fig. 6 as a function of x-ray dose. As shown, the ratio exhibits a similar behavior to that of the alpha diameters, changing rapidly with low doses and approaching an asymptotic value at ~20 Gy. Because the mean track diameter is proportional to the bulk etch rate (Eq. (3)), we infer that the observed track dependence on x-ray dose is produced primarily by this trend in the bulk etch rate.

$v_b(0)$ was also found using an independent method. If the initial (before etch) and final (after etch) masses of the sample are known, then the bulk etch rate is defined by

$$v_b(0) = \frac{\Delta m}{2A\rho t_{etch}}, \tag{6}$$

where the density $\rho = 1.30\ \mathrm{g/cm^3}$ and the area $A = 19.6\ \mathrm{cm^2}$. Using this formula, $v_b(0)$ was found to be $2.66 \pm 0.06\ \mu$m/h, which means that doses greater than 20 Gy result in an etch rate of approximately 1.80 $\mu$m/h. Other researchers[17] found in 1999 a value of 2.00 $\mu$m/h for $v_b(0)$, which suggests a change in the chemistry of CR-39 over the years. In fact, this ~33% difference in $v_b(0)$ explains the ~33% disagreement observed in Fig. 3 between the experiments performed in 1999 and the ones presented in this paper.

## IV. DATA ANALYSIS AND INTERPRETATION

As explained below, our interpretation of the data is that x-rays mainly change the bulk etch rate of the CR-39, which in turn alters the diameter of the tracks produced by etching. Physically, this behavior may occur due to the rupture of the bonds in the polymer, which reduces the possibility of $OH^-$ ions (from the NaOH) to react and extract parts of the molecules (etching). In addition, we have found that this

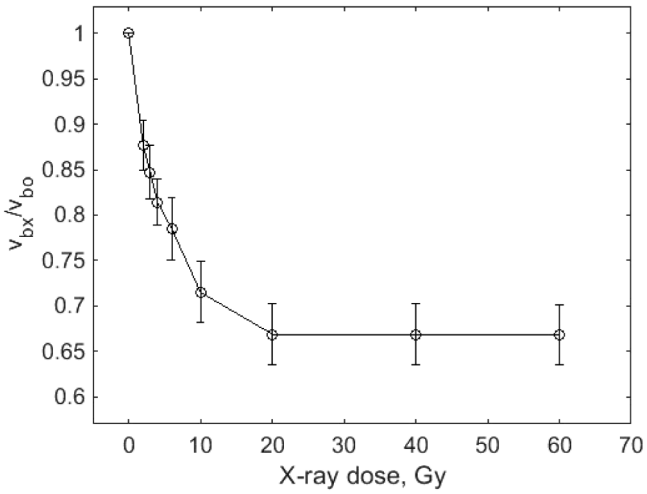


FIG. 6. Dimensionless bulk etch rate ratio between regions exposed and unexposed to x-rays as a function of dose. A reduction to an asymptotic value of $0.66 \pm 0.03$ at approximately 20 Gy is observed. This behavior is consistent with the change in track diameters shown in Fig. 5(a).

damage to the molecular structure depends on the x-ray dose applied, but not on the photon energy (Fig. 5(a)).

Experiments showed that the bulk etch rate was dependent on the dose. Therefore, the mean track diameter of alphas is a function of both particle energy and applied dose. Because both the mean track diameter and bulk etch rate were measured for different doses, we can evaluate the extent to which the track diameter reduction is explained by the bulk etch-rate change, by calculating

$$F(E,X) = \frac{D(E,X)}{D(E,0)} \Big/ \frac{v_b(X)}{v_b(0)}, \tag{7}$$

where E = energy and X = x-ray dose. This dimensionless parameter $F(E,X)$ turned out to differ from 1, as shown in Figure 7. This means that most of the x-ray effect is explained by the bulk etch rate change, but there is still some residual effect. A likely explanation is that the track etch rate ($v_t$, see Eq. (2)) also changes with changing x-ray dose.

The results, shown in Fig. 7, were found by dividing the results shown in Fig. 5(a) (normalized), by the results shown in Fig. 6. This figure might seem confusing at first sight because of its interesting energy dependence, but it can be mathematically explained as follows. Let us define $D(E,X)/D(E,0)$ as $D_{X/0}$ and $v_b(X)/v_b(0)$ as $v_{X/0}$. We know that $v_{X/0}$ is independent of incident particle energy, therefore, $D_{X/0}$ must be the term responsible for the energy dependence of $F(E,X)$. Figure 7 indicates that as the incident particle energy decreases, $D_{X/0}$ increases. Nevertheless, this increase only means that $D_{X/0}$ is closer to unity, and because $v_{X/0}$ behaves as in Fig. 6 then $F(E,X)$ will have values greater than one for low energies (E < 3 MeV) and values between zero and one for high energies.

An empirical model for Eq. (7) was found to quantify how much $v_t$ is changing

$$F(E,X) = 1 + \mathrm{erf}[aX]\left(b \exp\left[\frac{-(E-c)^2}{2d^2}\right] + e\right). \tag{8}$$

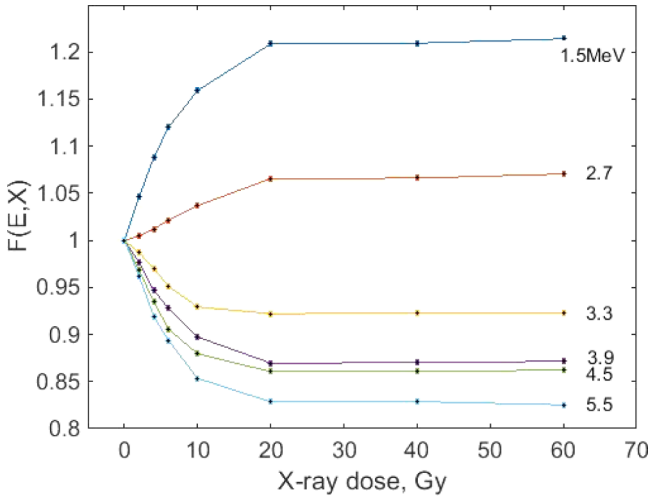


FIG. 7. $F(E,X)$ is a dimensionless parameter given by Eq. (7) which describes the residual effect due to changes in the track etch rate when CR-39 samples are exposed to x-rays. All CR-39 pieces were etched for 2 h in an 80 °C solution of 6 M NaOH. (The model is independent of $t_{etch}$.)

Here, a fit to the data gives $a = (95.83 \pm 4.79)10^{-3}$, $b = (37.37 \pm 1.79)10^{-2}$, $c = 1.589 \pm 0.079$, $d = 1.054 \pm 0.053$, and $e = (-16.27 \pm 0.81)10^{-2}$.

Additional experiments were also performed to confirm the assumption that $(dE/dx)_{elec}$ was not changing with x-ray dose. In these experiments, pieces of CR-39 were exposed to different x-ray doses after alpha particles were already deposited in the sample. These alphas-before-x-rays experiments still show a decrease in the mean track diameter, as expected, but the decrease is slightly less than in the x-rays-before-alphas methodology: $D_{X/0}$ was approximately 0.80× to 0.85× the values shown in Fig. 5(b). For example, if x-rays are deposited after alphas, the change in the mean track diameter for 2.7 MeV alphas asymptotes to −25% in the limit of large x-ray dose. These observations support the interpretation that most of the effect of x-rays on the response of CR-39 to alphas occurs during the etching process due to a change in the chemical structure of the polymer. This behavior is different from other observed environmental effects of the CR-39. It has been demonstrated, for example, that vacuum exposure longer than 16 h *before* proton irradiation on CR-39 results in a decrease in proton sensitivity, whereas no effect is observed for up to 67 h of vacuum exposure *after* proton irradiation.[19] Those results indicated that the properties of the plastic at the time of proton irradiation, rather than at etch time, produced the change in sensitivity with vacuum exposure.

In the context of many relevant experiments (for example ICF charged particle spectrometry), the x-ray dose will arrive immediately (on the order of 10 ns) before the alpha particles. The time required for the x-rays to change the molecular structure of the polymer remains unexplored; however, we do not expect the exposure time frame will significantly alter the observed effect. The properties of the plastic at etch time ($v_b$) appear to dominate the observed diameter reduction rather than the properties at the time of alpha deposition, and the etch process always occurs hours or days after the x-ray and alpha particle exposure. In the present study, the CR-39 was etched at least 1.5 h and at most 1 week after exposure to x-rays, and showed consistent results across this time period. Investigation of how the observed effect depends on the duration between the x-ray exposure and the etching of the CR-39, which can be several weeks depending on the application, remains as future work.

## V. CONCLUSIONS

A comprehensive study of how x-ray exposure affects the response of CR-39 nuclear track detector to 1–5.5 MeV alphas showed that the mean track diameter of alpha particles for regions exposed to x-rays decreased rapidly for doses of less than 20 Gy, but that it reached a constant value for greater doses. This variation in the track diameter is primarily due to a proportional change in the bulk etch rate of the piece. A dimensionless function $F(E,X)$ was found to quantify the residual effect on the tracks due to changes in track etch rate. These results represent the first quantitative measurements of x-ray effects on CR-39, which will be of great importance for researchers who make use of this nuclear track detector in environments with high levels of x-rays. Future studies to examine the effect on other charged particles, especially protons and deuterons, will be particularly important for experimental applications that record these particles.

## ACKNOWLEDGMENTS

The authors want to thank R. Frankel and E. Doeg for their help in processing of CR-39 data used in this work. This work was supported in part by the MIT UROP Office, U.S. Department of Energy (DOE) (Grant No. DE-NA0001857), National Laser Users Facility (DE-NA0002035), Laboratory for Laser Energetics (415935-G), and Lawrence Livermore National Laboratory (B600100).

[1]J. Nuckolls and L. Wood, "Laser compression of matter to super-high densities: Thermonuclear (CTR) applications," Nature **239**, 139–142 (1972).
[2]R. L. Fleischer, P. B. Price, and R. M. Walker, *Nuclear Tracks in Solids. Principles and Applications* (University of California Press, Berkeley, 1975).
[3]A. P. Fews and D. L. Henshaw, "High resolution alpha-particle spectroscopy using CR-39 plastic track detector," Nucl. Instrum. Methods Phys. Res. **197**, 517–529 (1981).
[4]H. A. Khan, R. Brandt, N. A. Khan, and K. Jamil, "Track-registration-and-development characteristics of CR-39 plastic track detector," Nucl. Tracks Radiat. Meas. **7**(3), 129–139 (1983).
[5]A. P. Fews, "Fully automated image analysis of etched tracks in CR-39," Nucl. Instrum. Methods Phys. **71**, 465 (1992).
[6]J. F. Ziegler, J. P. Biersack, and U. Littmark, *The Stopping and Range of Ions in Solids* (Pergamon Press, 1985), Vol. 1.
[7]N. Sinenian *et al.*, "The response of CR-39 nuclear track detector to 1–9 MeV protons," Rev. Sci. Instrum. **82**, 103303 (2011).
[8]F. H. Séguin *et al.*, "Advances in compact proton spectrometers for inertial-confinement fusion and plasma nuclear science," Rev. Sci. Instrum. **83**, 10D908 (2012).
[9]K. F. Chan, B. M. F. Lau, D. Nikezic, A. K. W. Tse, W. F. Fong, and K. N. Yu, "Simple preparation of thin CR-39 detectors for alpha-particle radiobiological experiments," Nucl. Instrum. Methods Phys. Res., Sect. B **263**(1), 290–293 (2007).
[10]Matiullah, S. Rehman, S. Rehman, and W. Zaman, "Discovery of new etchants for CR-39 detector," Radiat. Meas. **39**(3), 337–343 (2005).
[11]J. A. Frenje *et al.*, "Absolute measurements of neutron yields from DD and DT implosions at the OMEGA laser facility using CR-39 track detectors," Rev. Sci. Instrum. **73**, 2597 (2002).

[12]H. Sio, F. H. Séguin, J. A. Frenje, M. G. Johnson, A. B. Zylstra, H. G. Rinderknecht, M. J. Rosenberg, C. K. Li, and R. D. Petrasso, "A technique for extending by $\sim 10^3$ the dynamic range of compact proton spectrometers for diagnosing ICF implosions on the National Ignition Facility and OMEGA," Rev. Sci. Instrum. **85**, 11E119 (2014).
[13]F. H. Séguin, "Spectrometry of charged particles from inertial-confinment fusion plasmas," Rev. Sci. Instrum. **74**(2), 975 (2003).
[14]T. R. Boehly *et al.*, "Initial performance results of the OMEGA laser system," Opt. Commun. **133**, 495–506 (1997).
[15]G. Miller, E. I. Moses, and C. Wuest, "The National Ignition Facility: enabling fusion ignition for the 21st century," Nucl. Fusion **44**, 228–238 (2004).
[16]Track Analysis Systems Ltd. For more information, see http://www.tasl.co.uk/plastics.php.
[17]D. G. Hicks, "Charged-particle spectroscopy: a new window on Inertial Confinement Fusion," Ph.D thesis (Massachusetts Institute of Technology, 1999).
[18]D. Nikezic and K. N. Yu, "Formation and growth of tracks in nuclear track materials," Mater. Sci. Eng. R **46**, 51–123 (2004).
[19]M. J. E. Manuel, M. J. Rosenberg, N. Sinenian, H. Rinderknecht, A. B. Zylstra, F. H. Séguin, J. Frenje, C. K. Li, and R. D. Petrasso, "Changes in CR-39 proton sensitivity due to prolonged exposure to high vacuums relevant to the National Ignition Facility and OMEGA," Rev. Sci. Instrum. **82**, 095110 (2011).
[20]D. S. Hey, M. H. Key, A. J. Mackinnon, A. G. MacPhee, P. K. Patel, R. R. Freeman, L. D. V. Woerkom, and C. M. Castaneda, "Use of GafChromic film to diagnose laser generated proton beams," Rev. Sci. Instrum. **79**, 053501 (2008).